Published in final edited form as:
Neuroscience. 2011 November 24; 196: 251–264. doi:10.1016/j.neuroscience.2011.08.016.

DJ-1 KNOCK-DOWN IMPAIRS ASTROCYTE MITOCHONDRIAL FUNCTION

N. J. LARSEN[a], **G. AMBROSI**[b], **S. J. MULLETT**[a], **S. B. BERMAN**[a], and **D. A. HINKLE**[a,*]

[a]Department of Neurology, Pittsburgh Institute for Neurodegenerative Diseases, University of Pittsburgh School of Medicine, Pittsburgh, PA, USA

[b]Interdepartmental Research Center for Parkinson's Disease, IRCCS Neurological Institute "C. Mondino," Pavia, Italy

Abstract

Mitochondrial dysfunction has long been implicated in the pathogenesis of Parkinson's disease (PD). PD brain tissues show evidence for mitochondrial respiratory chain Complex I deficiency. Pharmacological inhibitors of Complex I, such as rotenone, cause experimental parkinsonism. The cytoprotective protein DJ-1, whose deletion is sufficient to cause genetic PD, is also known to have mitochondria-stabilizing properties. We have previously shown that DJ-1 is over-expressed in PD astrocytes, and that DJ-1 deficiency impairs the capacity of astrocytes to protect co-cultured neurons against rotenone. Since DJ-1 modulated, astrocyte-mediated neuroprotection against rotenone may depend upon proper astrocytic mitochondrial functioning, we hypothesized that DJ-1 deficiency would impair astrocyte mitochondrial motility, fission/fusion dynamics, membrane potential maintenance, and respiration, both at baseline and as an enhancement of rotenone-induced mitochondrial dysfunction. In astrocyte-enriched cultures, we observed that DJ-1 knock-down reduced mitochondrial motility primarily in the cellular processes of both untreated and rotenone treated cells. In these same cultures, DJ-1 knock-down did not appreciably affect mitochondrial fission, fusion, or respiration, but did enhance rotenone-induced reductions in the mitochondrial membrane potential. In neuron–astrocyte co-cultures, astrocytic DJ-1 knock-down reduced astrocyte process mitochondrial motility in untreated cells, but this effect was not maintained in the presence of rotenone. In the same co-cultures, astrocytic DJ-1 knock-down significantly reduced mitochondrial fusion in the astrocyte cell bodies, but not the processes, under the same conditions of rotenone treatment in which DJ-1 deficiency is known to impair astrocyte-mediated neuroprotection. Our studies therefore demonstrated the following new findings: (i) DJ-1 deficiency can impair astrocyte mitochondrial physiology at multiple levels, (ii) astrocyte mitochondrial dynamics vary with sub-cellular region, and (iii) the physical presence of neurons can affect astrocyte mitochondrial behavior.

Keywords

rotenone; mitochondria; dynamics; motility; fission; fusion

Mitochondrial dysfunction is linked to the pathogenesis of Parkinson's disease (PD) (Schapira, 2004; Büeler, 2009; Van Laar and Berman, 2009; Winklhofer and Haass, 2010; Zhu and Chu, 2010). For example, PD tissues show reduced mitochondrial respiratory chain Complex I activity in the substantia nigra pars compacta (Schapira et al., 1990), cerebral

*Corresponding author. Tel: +1-412-648-8364; fax: +1-412-648-7223. hinkleda@upmc.edu (D. A. Hinkle).

cortex (Parker et al., 2008), skeletal muscles (Blin et al., 1994), and blood platelets (Cooper et al., 1992; Haas et al., 1995). Cybrid experiments, in which mitochondrial DNA (mtDNA) from PD patients is introduced into mtDNA-depleted cells, show transferred deficiencies in mitochondrial Complex I activity and respiratory capacity (Trimmer and Bennett, 2009; Esteves et al., 2010). In addition, direct molecular links between PD and mitochondrial dysfunction have been established by the discovery of disease-causing mutations in genes that encode proteins that modulate mitochondrial function: PINK1 (phosphate and tensin homolog induced putative kinase 1), parkin, and DJ-1 (Kitada et al., 1998; Bonifati et al., 2003; Paisén-Ruíz et al, 2004; Knott and Bossy-Wetzel, 2008; Van Laar and Berman, 2009; Burbulla et al., 2010).

DJ-1 was first linked to PD when deletional mutations in its gene were discovered to cause a familial, early-onset form of the disease (Bonifati et al., 2003). DJ-1 is a cyto-protective protein that acts to promote mitochondria-stabilizing anti-oxidant and anti-apoptotic mechanisms in non-astrocytic primary cells and cell lines (Canet-Avilés et al, 2004; Taira et al., 2004; Junn et al., 2005; Xu et al., 2005; Zhou and Freed, 2005; Clements et al., 2006; Aleyasin et al., 2007; Liu et al., 2008; Blackinton et al., 2009). DJ-1 deficiency has been shown to impair mitochondrial connectivity, fusion rates, membrane potential ($\Delta\Psi$ m), respiratory capacity, and reactive oxygen species (ROS) buffering in non-astrocytic cells *in vitro* (Ved et al., 2005; Blackinton et al., 2009; Hao et al., 2010; Irrcher et al., 2010; Krebiehl et al., 2010; Thomas et al., 2011).

We have observed that DJ-1 is over-expressed in reactive astrocytes, but not neurons, in PD and other neuro-degenerative disorders (Rizzu et al., 2004; Mullett et al., 2009). This prompted us to consider the possibilities that (i) astrocytic DJ-1 may function to protect astrocytes and surrounding neurons against the progression of sporadic PD, and that (ii) DJ-1 deletion in genetic PD may permit neurodegeneration primarily because of absent astrocytic expression. We tested this latter possibility in neuron–astrocyte co-cultures and discovered that small interfering RNA (siRNA)-mediated DJ-1 knock-down astrocytes were significantly impaired in their capacity to protect neurons against rotenone and other Complex I inhibitors (Mullett and Hinkle, 2009, 2011). This finding may be relevant to PD because pharmacologic inhibition of Complex I using 1-methyl-4-phenyl-1,2,3,6-tetrahydropyridine (MPTP) or pesticides (rotenone) causes mitochondrial dysfunction and experimental parkinsonism (Langston et al., 1984; Ballard et al., 1985; Betarbet et al., 2000; Panov et al., 2005; Cannon et al., 2009). In addition, human occupational exposure to pesticides, including rotenone, is epidemiologically-linked with an increased risk for PD (Ascherio et al., 2006; Brown et al., 2006; Sherer et al., 2007; Gash et al., 2008; Tanner et al., 2010). Rotenone has also been shown to reduce mitochondrial motility, $\Delta\Psi$m, and respiration, and to alter mitochondrial morphology, sub-cellular distribution, and fission/fusion balance in non-astrocytic cells (Pham et al., 2004; Barsoum et al., 2006; Benard et al., 2007; Koopman et al., 2007; Yadava and Nicholls, 2007; Borland et al., 2008; Mortiboys et al., 2008; Van Laar and Berman, 2009; Arnold et al., 2011).

Since DJ-1 is linked to the maintenance of normal mitochondrial physiology in a variety of cell types, and since its knock-down impairs astrocyte-mediated neuro-protection against Complex I inhibitors, we hypothesized that DJ-1 deficiency would broadly impair astrocyte mitochondrial functioning. Although little is known about this concept in this cell type, one group recently showed that astrocytes cultured from DJ-1 knockout mice exhibited impaired baseline $\Delta\Psi$m (Ashley et al., 2009). Therefore, we hypothesized that DJ-1 knock-down would impair astrocyte mitochondrial motility and fission/fusion dynamics, $\Delta\Psi$m maintenance, and respiration under experimental conditions in which DJ-1 modulated, astrocyte-mediated neuroprotection is known to be weakened.

EXPERIMENTAL PROCEDURES

Astrocyte cultures, siRNA transfections, and experimental treatments

Primary astrocyte-enriched cultures were produced as we have previously described (Mullett and Hinkle, 2009, 2011). Briefly, astrocytes were prepared from postnatal day 1 CD1 mouse cerebral cortex tissues by dissociation into Neurobasal media (Invitrogen, Carlsbad, CA, USA) containing 10% fetal calf serum (FCS, HyClone, Logan, UT, USA) and 1× antibiotic-antimycotic (ABAM, Invitrogen). The plating density was 7.3×10^4 trypan blue-excluding cells/cm^2. The cultures were fed with Dulbecco's modified Eagle media (DMEM)/F12 (Sigma, St. Louis, MO, USA)/FCS/ ABAM for the first week, then maintained in DMEM/F12/ABAM containing 10% calf serum (CS, HyClone). Monolayers prepared in this fashion contained ~97% glial fibrillary acidic protein (GFAP) immunoreactive astrocytes. Neuron–astrocyte contact co-cultures were prepared exactly as described in our previous publications (Mullett and Hinkle, 2009, 2011).

DJ-1 knock-down was effected by siRNA transfections over astrocyte days *in vitro* (DIV) 10–13 using methods that we have previously described and validated (Mullett and Hinkle, 2009). Briefly, a 21 nucleotide double-stranded anti-mouse DJ-1 siRNA of sequence AGG CGC GGC TGC AGT CTT TAA (siDJ#2, Invitrogen) was used to suppress DJ-1 protein to ~5% of endogenous levels (DJ-1 knock-down). We have previously established that siDJ#2-induced DJ-1 knock-down persists throughout the entire experimental period, and that its levels in astrocytes, and its physiological effects in our co-culture system, are fully reversible by co-transfection with a non siDJ#2-targeted mouse DJ-1 rescue cDNA (Mullett and Hinkle, 2009). Since these controls have already been published for the same *in vitro* system that is used here, and since they establish DJ-1 levels prior to and regardless of subsequent toxin treatment and experimentation, we did not repeat them here. A non-silencing siRNA of sequence AAT TCT CCG AAC GTG TCA CGT (siNS, Invitrogen) was used as a transfection control (control). The siNS had no sequence matches on Basic Local Alignment Search Tool (BLAST) analysis, and no effect on DJ-1, α-tubulin, or β-actin protein levels, as we have previously published (Mullett and Hinkle, 2009, 2011).

At 20 DIV the astrocytes were exposed to rotenone (Sigma) and/or p-trifluoromethoxy carbonyl cyanide phenyl hydrazone (FCCP, a respiratory uncoupler, Sigma) for up to 72 h. These agents were dissolved in dimethyl sulfoxide (DMSO) prior to dilution in Neurobasal/1× B27 antioxidant free (Invitrogen)/1× ABAM and compared to vehicle-only control medias.

Whole-cell mitochondrial motility

Whole-cell mitochondrial motility was assessed in live astrocytes using mitochondria-targeted red fluorescent protein (mtDsRed2) to identify and track the organelles using a modification of our previously described methods (Arnold et al., 2011). Briefly, astrocytes were transfected with plasmids containing a mitochondrial localization sequence from cytochrome c oxidase subunit VIII inserted upstream of DsRed2 cDNA (Clontech, Mountain View, CA, USA). mtDsRed2 plasmid was incubated in a 2 μg DNA:3 μl Transfectin Lipid Reagent (Bio-Rad, Hercules, CA, USA) ratio to form transfection complexes, then applied to the astrocyte monolayers in DMEM/F12/CS/ ABAM for 4 h at 37 °C. The cells were then washed with fresh media, allowed to recover for 48 h, then exposed to rotenone vs. vehicle for 24 h.

Treated cells were imaged live at room temperature for 5 m using an inverted fluorescence microscope (Olympus IX71) and SPOT Advanced software version 4.6 (Olympus America, Center Valley, PA, USA). One cell field per treatment per replicate experiment was randomly identified and excited at 543 nm to visualize the mtDsRed2-labeled mitochondria.

Images were obtained every 10 s over 5 m. Mitochondrial motility was assessed from the sequentially collected images using ImageJ self-initializing, two-dimensional particle tracking analysis software from the National Institutes of Health (Sbalzarini and Koumoutsakos, 2005). Individual mtDsRed2+ mitochondria ("particles") were identified automatically from the initial image when their intensity was detected above a pre-set background cutoff. A threshold radius was then automatically set around each particle by the software. A mitochondrial movement, or "trajectory," was recorded when of any portion of any mtDsRed2+ particle crossed its threshold radius from the previous image. Data were collected for all particles as trajectories per particle (movements per mitochondrion) through the entire series of images. Each individual data point was calculated as the average number of trajectories per mitochondrion from three different astrocytes from the same culture dish. This method allowed us to measure the majority of mitochondrial movements that occurred in the three-dimensional cell. Movements that occurred in line with the microscope objective could not be detected; however, we estimate that these movements had a negligible impact on our outcomes.

Regional mitochondrial motility

These assessments were also performed in live astrocytes using a modification of our previously described methods (Berman et al., 2009). Astrocytes were again transfected with mtDsRed2 plasmids to identify all mitochondria. However, the astrocytes were also transfected with a plasmid containing mitochondria-targeted photoactivatable green fluorescent protein (mtPAGFP) cDNA (provided to S.B. by R. Youle). Confocal microscopic fields containing astrocytes expressing mtDsRed2 were randomly identified, and then single whole cells within those fields were randomly selected for study. Within each cell a 405 nm laser pulse was used to photoactivate the PAGFP to generate a region of interest (ROI) in one cellular process and at one location within the cell body (both randomly determined). Laser intensity was set at 1% to prevent phototoxicity and was maintained throughout the experiments. The ROI was visible as yellow-green mitochondria when excited at 488 nm. Data collection began immediately following laser photoactivation by dual-excitation image capture every 10 s for 15 m at 37 °C in buffered Minimal Essential Media pH 7.4 supplemented with 2% GlutaMAX (Invitrogen), 20 mM HEPES, 33 mM glucose, and 1 mM sodium pyruvate.

Motility was assessed as mitochondrial "egress" events and "mobile proportions" using the same image series. Egress events were manually counted in a treatment-blinded fashion through the sequential images. One egress event was scored when any mitochondrion was observed to cross an ROI boundary. Egress events involving an ROI were normalized to the total number of photoactivated mitochondria counted within that ROI (as identified by ImageJ particle detection software). Mobile proportions were calculated by normalizing the number of photoactivated mitochondria within an ROI that changed position at least once between any two sequential images to the total number of photoactivated mitochondria within that ROI. For this assessment, once a mitochondrion moved it was no longer considered in subsequent images. Each data point was calculated as the average number of egress events/mitochondrion or mobile proportions from three different astrocytes in the same culture dish. This single-plane method did not allow us to account for the three-dimensional nature of the cell. However, it was necessary to assess sub-cellular regions in a manner that limited phototoxicity as the time-lapse images were collected.

Regional mitochondrial fission and fusion

Mitochondrial fission and fusion were manually assessed in a treatment-blinded fashion from the same images generated in the previous section. A fission event was counted when a single photoactivated mitochondrion was observed to split into two or more fragments over

sequential images. Fission events were counted within or outside of the ROI, and thus were not dependent on mitochondrial motility. Fission events were normalized to the total number of mitochondria within the adjacent ROI, and each data point was calculated as the average number of fission events/mitochondrion from three different astrocytes in the same culture dish.

A fusion event was counted when a photoactivated mitochondrion (green fluorescent) from within a source ROI was observed to share its PAGFP contents with a non-photoactivated mitochondrion (red fluorescent) to form a single, yellow-fluorescent mitochondrion. Fusion events were counted within or outside of the ROI, but were dependent upon motility (i.e. green fluorescent mitochondria needed to move out of the ROI to fuse with red fluorescent mitochondria, or vice versa). Therefore, the number of fusion events was normalized to egress events within the source ROI. Each data point was calculated as the average number of fusion events/egress event from three different astrocytes from the same culture dish.

Mitochondrial membrane depolarization

The $\Delta\Psi m$ was assessed in live astrocytes using 5,5′,6,6′-tetra-chloro-1,1′,3,3′-tetraethylbenzimidazolylcarbocyanine iodide (JC-1; Invitrogen, Carlsbad, CA, USA). JC-1 is a cationic, dual-emission fluorescent dye that accumulates as red fluorescent J-aggregates within polarized, internal negative mitochondria. Depolarization of the $\Delta\Psi m$ results in J-aggregate release as green fluorescent monomers. Thus, a fluorescence shift from red to green, or a decrease in the red/green fluorescence ratio, is indicative of $\Delta\Psi m$ depolarization (Reers et al., 1991, 1995; Smiley et al., 1991; White and Reynolds, 1996).

Astrocytes were incubated with 1 μM JC-1 dye for 30 m at 37 °C to produce maximal dye absorption with minimal background. The cells were then rinsed with media and placed in a non-CO_2 incubation chamber at 37 °C for live imaging using a confocal microscope (Olympus IX81) with Fluoview FV10-ASW 2.0 software (Olympus). One cell field per treatment per replicate experiment was randomly identified and excited at 488 nm. The whole-field fluorescence intensities for both aggregate (590 nm, red) and monomeric (527 nm, green) JC-1 were equalized at time 0 to establish a baseline. Treatments were then initiated and images were acquired every 30 s for 2 h to calculate red/green fluorescence intensity ratios.

Mitochondrial respiration and glycolytic flux

Real-time mitochondrial respiration and glycolytic flux were simultaneously assessed in live astrocytes using a Seahorse Bioscience XF-24 Analyzer (Seahorse Bioscience, Billerica, MA, USA) (Ferrick et al., 2008; Gerencser et al., 2009). Oxygen consumption rates (OCR) were calculated as a measure of aerobic respiration, and extracellular acidification rates (ECAR) were calculated as a measure of lactic acid production in anaerobic glycolysis. To do this, astrocytes were cultured in Seahorse 24-well plates, transfected to manipulate DJ-1 as described above, then incubated in unbuffered DMEM pH 7.4 at 37 °C in a non-CO_2 incubator for 30 min. Experimental agents were loaded into the Seahorse injection ports and the probes for detection were calibrated by the XF24 analyzer. The astrocyte-containing culture plates were then loaded into the instrument and baseline OCR and ECAR measurements were collected. The experimental agents (rotenone alone or rotenone followed by FCCP) were then injected and OCR and ECAR measurements were collected every 8 m from 0 to 1 h, 6 to 7 h, and 24 to 25 h.

The OCR and ECAR measurements from each well were then normalized in two ways. First, the metabolic measurements from each well were normalized to the number of astrocytes in the same well. To do this, quantitative GFAP in-cell Western blots were

employed using the Odyssey imager, as we have described and validated (Mullett and Hinkle, 2011). Briefly, the astrocytes were lightly fixed with 4% paraformaldehyde, blocked, and probed with a rabbit anti-GFAP primary polyclonal antibody (Dako, Glostrup, Denmark) at 1:5000. An Alexa 680-conjugated anti-rabbit secondary antibody (Invitrogen) was then applied at 1:5000. Infrared signal, which correlated with the amount of GFAP (number of astrocytes) in that well, was then quantified. Background signal was removed and the average of three to four wells per treatment was used to generate each single data point. Second, each average OCR/GFAP and ECAR/GFAP value was normalized to vehicle control at each time point to account for minor reductions in basal rates that occurred as time progressed through the experiments. All assessments were performed within the linear ranges of the Seahorse and Odyssey machines.

Statistics

Independent cultures, transfections, and treatments were used for each replicate experiment. Since the effect of DJ-1 deficiency was always sought as the primary outcome, statistical comparisons were made between same-treatment/same-time control and DJ-1 knock-down groups in five to six replicate experiments using paired *t*-tests. Statistical significance was set at $P<0.05$.

RESULTS

DJ-1-knock-down impaired astrocyte mitochondrial motility

We hypothesized that DJ-1 knock-down would impair astrocyte mitochondrial motility at baseline, and as an enhancement of rotenone-induced impairment. We first approached this hypothesis by assessing mitochondrial movements in whole, live-imaged control, and DJ-1 knockdown astrocytes. In untreated cells, DJ-1 knock-down reduced mitochondrial motility relative to control (Fig. 1A). In control astrocytes, rotenone treatment reduced mitochondrial motility to a similar degree. However, there was no evidence for additive or synergistic effects for combined DJ-1 knock-down and rotenone treatment.

Visual analysis of sequential images collected from the whole-cell experiments suggested that mitochondrial motility may be affected in a region-selective manner. Therefore, we proceeded to separately evaluate astrocyte cellular processes and cell bodies for mitochondrial motility in confocal microscope images by treatment-blinded manual counts of mitochondrial ROI egress events (Fig. 2A, B; Suppl. Fig. 1) and mobile proportions (Fig. 2C, D). We found that mitochondrial ROI egress in DJ-1 knock-down astrocyte processes was significantly reduced compared to control processes in both untreated and 20 nM rotenone treated cells (Fig. 2A; Suppl. Figs. 2 and 3). High-dose (40 nM) rotenone treatment produced a slowing trend in control process mitochondrial egress that approached the level seen with DJ-1 knock-down. In the cell body, untreated and 20 nM rotenone treated control and DJ-1 knock-down astrocytes exhibited similar levels of mitochondrial ROI egress (Fig. 2B). However, in the presence of 40 nM rotenone, mitochondrial ROI egress in the DJ-1 knockdown astrocyte cell body was significantly reduced compared to controls.

The mitochondrial ROI mobile proportion assessments produced similar findings to the egress analysis. In the astrocyte processes, DJ-1 knock-down significantly reduced the mitochondrial mobile proportion relative to controls under all treatment conditions (Fig. 2C). However, in the astrocyte cell body, DJ-1 knock-down only reduced the mobile fraction in the presence of 40 nM rotenone (Fig. 2D).

DJ-1 knock-down reduced mitochondrial fission in high-dose rotenone treated astrocyte processes, but did not affect mitochondrial fusion

Since DJ-1 knock-down impaired astrocyte mitochondrial motility, we proceeded to assess mitochondrial fission and fusion. We hypothesized that DJ-1 knock-down would stimulate the mitochondrial fission/fragmentation rate and reduce the fusion rate.

Our assessments of fission were based on visualized splitting/fragmentation of any PAGFP+ or DsRed2+ mitochondrion over sequential confocal images (Suppl. Fig. 4). There was a trend towards reduced mitochondrial fission in the DJ-1 knock-down astrocytes in both sub-cellular regions (Fig. 3). However, this difference only became significant in the cellular processes of astrocytes treated with 40 nM rotenone.

Our assessments of fusion were based on visualized mixing of mitochondrial PAGFP (from within the laser-photoactivated ROIs) and DsRed2 from a non-photoactivated mitochondrion (from outside of the ROIs) over sequential confocal images (Suppl. Fig. 5). We did not attempt to identify PAGFP-PAGFP or DsRed2-DsRed2 mitochondrial fusion events. We did not see significant differences in mitochondrial fusion between the DJ-1 knock-down and control astrocytes at baseline or after treatment with rotenone in either sub-cellular region (Fig. 4).

The presence of contact co-cultured neurons altered the effects of astrocytic DJ-1 knock-down and rotenone treatment on astrocyte mitochondrial dynamics

Astrocytic DJ-1 knock-down impairs the capacity of astrocytes to support contact co-cultured neurons against 20 – 40 nM rotenone-induced death (Mullett and Hinkle, 2009, 2011). Given the above results in astrocyte-enriched cultures, and the capacity of our confocal/manual counting methods to easily distinguish astrocytic from neuronal mitochondria, we studied the same astrocyte mitochondrial dynamics parameters in the presence of contact co-cultured neurons.

In the co-cultures, there was a trend towards reduced astrocyte mitochondrial ROI egress in untreated DJ-1 knock-down processes and cell bodies, relative to controls, but the effect of DJ-1 knock-down did not reach statistical significance under any condition of treatment (Fig. 5A, B). In the same co-cultures, the astrocyte mitochondrial mobile proportion was significantly reduced only in untreated DJ-1 knock-down processes relative to controls (Fig. 5C, D). Further, astrocytic DJ-1 knock-down did not affect mitochondrial fission under any conditions of treatment (Fig. 5E, F). However, astrocytic DJ-1 knock-down did significantly reduce mitochondrial fusion in 20 nM rotenone treated astrocyte cell bodies, relative to controls, an effect that was obscured at 40 nM rotenone by a similar reduction in fusion induced by the toxin alone (Fig. 5G, H).

DJ-1 knock-down enhanced rotenone-induced astrocyte ΔΨm depolarization

We hypothesized that DJ-1 knock-down would destabilize astrocyte ΔΨm under both basal and rotenone-stressed conditions. A subtle depolarization of the ΔΨm was observed in untreated DJ-1 knock-down and control astrocytes over a monitoring period of 2 h, but no significant differences were seen between the two DJ-1 conditions (Fig. 6, “No FCCP” curves). The ΔΨm destabilizing agent FCCP was then used to produce maximal ΔΨm depolarization, but again no differences were seen between the DJ-1 knock-down and control astrocytes (Fig. 6, “500 nM FCCP” curves).

Astrocytes were next exposed to 20 nM and 40 nM rotenone over a period of 2 h to assess for ΔΨm changes (Fig. 7). As expected, rotenone stimulated ΔΨm depolarization in the control astrocytes. As hypothesized, DJ-1 knock-down significantly accelerated and

enhanced the magnitude of ΔΨm depolarization beyond control levels at each rotenone dose. These assessments were performed solely in the astrocyte-enriched cultures because our methods were not capable of distinguishing neuronal ΔΨm effects from astrocyte ΔΨm effects in the contact co-cultures.

DJ-1 knock-down did not impair astrocyte mitochondrial respiration

We hypothesized that astrocytic DJ-1 knock-down would (i) impair baseline mitochondrial respiration, (ii) augment rotenone-induced respiratory impairment, and (iii) limit FCCP-enhanced uncoupled respiration, relative to control astrocytes. We also hypothesized that DJ-1 knock-down-induced impairments in respiration would stimulate a shift to glycolysis.

We measured the OCR in live astrocytes as an indicator of mitochondrial respiration. There were no significant basal differences in OCR observed between the DJ-1 knock-down and control astrocytes (Fig. 8). As expected, the addition of rotenone reduced OCR (40 nM > 20 nM) by the first time point tested (8 m, Fig. 8A). This reduction was maintained over 24 h of treatment (Fig. 8B). However, the rotenone-induced OCR reduction was not enhanced by DJ-1 knock-down. To further test the effects of DJ-1 knock-down, we maximized the OCR by exposing the astrocytes to FCCP (500 nM), a mitochondrial respiratory chain uncoupler (Fig. 8A). As expected, the addition of FCCP increased the OCR by the first time point tested (24 m) under all rotenone treatment conditions, and rotenone limited this stimulation in a dose-dependent fashion. However, there were again no significant differences in OCR observed between the DJ-1 knock-down and control astrocytes.

We simultaneously measured the ECAR, which varies directly with lactate production as an indicator of glycolytic flux. We observed no significant basal differences in ECAR between the DJ-1 knock-down and control astrocytes (Fig. 9). As expected, the addition of both rotenone (20 nM = 40 nM) and FCCP (500 nM) increased the ECAR. However, there was again no significant difference in ECAR between the DJ-1 knock-down and control astrocytes under any conditions of treatment. The OCR and ECAR assessments were performed solely in the astrocyte-enriched cultures because our methods were not capable of distinguishing neuron effects from astrocyte effects in the contact co-cultures.

DISCUSSION

We have recently shown that DJ-1 deficient astrocytes are physiologically impaired based on their reduced capacity to protect co-cultured neurons against rotenone (Mullett and Hinkle, 2009, 2011). The mechanism(s) involved in this phenomenon, however, remain unknown. Since there are published links between normal DJ-1 expression and preserved mitochondrial function in other cell types, we hypothesized that astrocytic DJ-1 knock-down would adversely affect multiple aspects of astrocyte mitochondrial physiology: motility, fission, fusion, ΔΨm stability, and respiration. We discovered that DJ-1 knock-down reduced astrocytic mitochondrial motility and ΔΨm. However, the most relevant finding to our model was that DJ-1 knock-down reduced mitochondrial fusion under the same conditions of neuron–astrocyte co-culture and rotenone treatment in which astrocyte-mediated neuroprotection is known to be impaired.

We first addressed the effects of DJ-1 knock-down on mitochondrial motility in astrocyte-enriched cultures. Mitochondria move along cytoskeletal networks to maintain their distribution throughout the cell (Heggeness et al., 1978). In neurons, mitochondria are transported in antero-grade and retrograde fashion along axon and dendrite cytoskeletal elements to promote synaptic function (Hollenbeck and Saxton, 2005; Okamoto and Shaw, 2005; Berman et al., 2009). In fact, the neurotoxic mechanism of rotenone may involve cytoskeletal disruption (Feng, 2006; Sanchez et al., 2008), and both acute and chronic

treatments with rotenone can reduce mitochondrial motility *in vitro* (Pham et al., 2004; Koopman et al., 2007; Borland et al., 2008). To date, mitochondrial motility has not been formally studied in astrocytes, or in relationship to DJ-1 expression. Therefore, because DJ-1 deficiency adversely affects astrocyte physiology, particularly in the presence of rotenone, we hypothesized that DJ-1 knock-down would reduce astrocyte mitochondrial motility in untreated cells and as an augmentation of the rotenone effect.

We initially approached this question using whole-cell assessments of mitochondrial motility in live astrocytes. We found that astrocytic DJ-1 deficiency modestly, but significantly, reduced mitochondrial motility in untreated cells. Rotenone treatment also reduced motility to a similar degree in control astrocytes, but there was no evidence for an additive or synergistic effect with DJ-1 knock-down. Visual analysis of the source images suggested that the changes in mitochondrial motility varied with sub-cellular region. Therefore, we addressed this question using a second type of analysis: we counted mitochondrial ROI egress events and mobility proportions in cellular processes and cell bodies using sequential confocal microscope images. Analysis of these data confirmed our suspicions: DJ-1 knock-down was the principal driving force behind the impairment in mitochondrial motility, and this impairment occurred primarily in the astrocyte processes. Interestingly, although there were similarities of pattern between the two sub-cellular regions, the reduction of cell body mitochondrial motility in response to DJ-1 knockdown was not significant until the cells were treated with high-dose rotenone. These findings suggest that mitochondrial trafficking in the astrocyte cell body is not as sensitive to DJ-1 knock-down as it is in the cellular processes, and that further stress (i.e. rotenone) is required to bring about significant motility changes in that sub-cellular region.

We next assessed the enriched astrocyte cultures for changes in mitochondrial fission and fusion under the same experimental conditions, since maintaining a balance between these processes also contributes to the preservation of normal cellular function (Westermann, 2002; Li et al., 2004; Knott and Bossy-Wetzel, 2008; Büeler, 2009; Van Laar and Berman, 2009; Burbulla et al., 2010). Mitochondrial fission, which results in the splitting of a single organelle into one or more new mitochondria, prevents abnormal elongation (and related senescence), enhances proliferation and distribution, and, potentially, allows for the isolation and removal of abnormally functioning portions of the organelle. Mitochondrial fusion, which results when two separate organelles fuse their matrix contents, allows for the transfer of metabolic contents, the recombination and maintenance of mitochondrial DNA, and the preservation of biochemical and electrical connectivity between organelles. Both DJ-1 and rotenone have been reported to modulate each of these processes in non-astrocytic cells. For example, DJ-1 deficiency has been shown to enhance mitochondrial fragmentation and to reduce mitochondrial fusion *in vitro*, probably by a pathway that is parallel to PINK1/parkin (Blackinton et al., 2009; Irrcher et al., 2010; Kamp et al., 2010; Thomas et al., 2011). In addition, rotenone has been shown to promote mitochondrial fragmentation *in vitro* (Barsoum et al., 2006; Mortiboys et al., 2008) and to simultaneously alter the rates of fission and fusion in neuronal processes (Arnold et al., 2011).

We therefore hypothesized that DJ-1 knock-down and rotenone treatment would each independently stimulate fission and reduce fusion in the astrocyte mitochondria, and that DJ-1 knock-down would amplify the rotenone effect when the two conditions were studied simultaneously. Our assessments in astrocyte-enriched cultures showed a trend towards reduced fission in both the cellular processes and cell bodies of DJ-1 knock-down astrocytes, but this effect was only significant in the processes when highly neurotoxic doses of rotenone (40 nM, based on our co-culture studies) were used. Rotenone treatment alone had no significant effect on fission in either sub-cellular region, and mitochondrial fusion

was not significantly affected by either DJ-1 knock-down or rotenone treatment in either sub-cellular region.

The more prominent reductions in mitochondrial motility and fission within the astrocyte processes were very interesting to us because these are the cellular regions that interact with neurons and blood vessels to modulate synaptic signaling and neurovascular coupling *in vivo* (Volterra and Meldolesi, 2005; Oberheim et al., 2006, 2009). We therefore assessed the same mitochondrial dynamics parameters in astrocyte processes and cell bodies in neuron–astrocyte contact co-cultures. Relative to the astrocyte-enriched cultures, the presence of co-cultured neurons blunted the baseline astrocyte mitochondrial egress rates, but not the mobile proportions, in both sub-cellular regions. In the co-cultures, astrocytic DJ-1 knock-down again significantly reduced mitochondrial motility in the untreated astrocyte processes. However, this effect was lost when the co-cultures were treated with rotenone, which itself more robustly impaired astrocyte mitochondrial motility here than in the astrocyte-enriched cultures. We therefore concluded that astrocyte mitochondrial motility is not relevant to the mechanism of DJ-1 modulated, astrocyte-mediated neuroprotection against rotenone in our *in vitro* system.

The astrocyte mitochondrial fusion analysis, however, was quite remarkable in the neuron–astrocyte co-cultures. Similar to the astrocyte-enriched cultures, no significant findings were made in the astrocyte processes. However, unlike the astrocyte-enriched cultures, in the co-cultures astrocytic DJ-1 knock-down induced a large and significant reduction in astrocyte cell body mitochondrial fusion in the presence of 20 nM rotenone. This effect was not present in untreated cultures, where fusion rates were baseline and equal for each type of astrocyte, and was obscured in cultures treated with 40 nM rotenone by a suppressive effect of the toxin itself. This was a particularly interesting set of findings because it exactly paralleled the pattern that we have repeatedly seen regarding DJ-1 modulated, astrocyte-mediated neuroprotection in the same co-culture system: (i) baseline and equal numbers of untreated surviving neurons cultured in contact with control and DJ-1 knock-down astrocytes, (ii) maximal separation between the survival of neurons co-cultured with control astrocytes (near-baseline) and DJ-1 knock-down astrocytes (low survival) after treatment with 20 nM rotenone, and (iii) low-level neuronal survival with a modest benefit provided by control relative to DJ-1 knock-down astrocytes after treatment with 40 nM rotenone (Mullett and Hinkle, 2009, 2011). We do yet know if these finding are mechanistically relevant to astrocyte-mediated neuroprotection in our *in vitro* system, or how DJ-1 knock-down and rotenone treatment may combine to reduce astrocyte mitochondrial fusion, but the parallels with our previous work are intriguing and worth further investigation.

The mitochondrial fission analysis demonstrated that rotenone appeared to be the main driving force for reduced astrocyte process and cell body fission rates in the neuron–astrocyte co-cultures, whereas astrocytic DJ-1 knockdown had no apparent effect. This was very different from the astrocyte-enriched cultures, in which rotenone had essentially no effect. We therefore concluded that DJ-1 knock-down either had no significant effect on fission, or only a small effect that was obscured by the more robust action of the rotenone. In either case, the lack of a distinguishable DJ-1 knock-down effect in the co-cultures also eliminated astrocyte mitochondrial fission as a viable mechanistic consideration for astrocyte-mediated neuro-protection in our system.

We also studied the astrocyte $\Delta\Psi m$ with the hypothesis that DJ-1 knock-down would enhance rotenone-induced depolarization. As a mitochondrial respiratory chain Complex I inhibitor, rotenone depolarizes the $\Delta\Psi m$ by blocking electron flow and reducing proton gradient formation across the inner mitochondrial membrane (Radad et al., 2006; Kim et al., 2007). DJ-1 deficiency has also been shown to depolarize the baseline $\Delta\Psi m$ in astrocytes

and fibroblasts cultured from DJ-1 knockout mice, and small hairpin RNA-mediated DJ-1 knock-down has produced similar results in non-astrocytic cell lines (Ashley et al., 2009; Krebiehl et al., 2010; Thomas et al., 2011). Since the combination of DJ-1 knock-down and rotenone treatment has never been assessed in astrocytes, we did so in astrocyte-enriched cultures under our previously-established experimental conditions (Mullett and Hinkle, 2009, 2011). We found that DJ-1 knock-down significantly enhanced rotenone-induced $\Delta\Psi m$ depolarization, both in terms of rate of development and magnitude. However, we found no evidence for baseline or FCCP-induced differences in $\Delta\Psi m$ between control and DJ-1 knock-down astrocytes. We suspect that the disparity between the effects of rotenone and FCCP was due to the capacity of FCCP to maximally reduce $\Delta\Psi m$. Thus, we concluded that DJ-1 knock-down may impair $\Delta\Psi m$ under conditions in which astrocyte-mediated neuroprotection is weakened (Mullett and Hinkle, 2009). However, we recognize that this conclusion is limited by the facts that we could not perform these assessments in neuron–astrocyte contact co-cultures (for technical reasons) and that similar experimental conditions did not produce changes in mitochondrial respiration (discussed below).

Our findings that DJ-1 deficiency induced abnormalities in mitochondrial dynamics and $\Delta\Psi m$ also prompted us to study astrocyte mitochondrial respiration. Both rotenone treatment (Panov et al., 2005; Radad et al., 2006; Sherer et al., 2007; Yadava and Nicholls, 2007) and DJ-1 deficiency (Hao et al., 2010; Irrcher et al., 2010; Krebiehl et al., 2010) have been shown to reduce mitochondrial respiration, but the combination has never been tested in astrocytes. We hypothesized that DJ-1 knock-down would impair astrocyte respiration (i) at baseline, (ii) as an enhancement of rotenone-induced respiratory impairment, and (iii) as a limiting factor to maximal FCCP-uncoupled respiratory stimulation. We also hypothesized that a DJ-1 knock-down-induced respiratory impairment would force a shift to glycolysis, a process that is well-described in astrocytes (Ouyang and Giffard, 2004; Radad et al., 2006). We found that rotenone (40 nM > 20 nM) reduced, and FCCP stimulated, astrocyte respiration. Likewise, both rotenone and FCCP stimulated a glycolytic shift. Each of these results was expected. However, there was no effect of DJ-1 knock-down on any of these parameters. Therefore, we concluded that DJ-1 knockdown did not alter mitochondrial respiration under conditions that are relevant to astrocyte-mediated neuroprotection against rotenone. Whether or not these findings obviate our $\Delta\Psi m$ results is unclear, since others have reported similar disconnections between rotenone-induced $\Delta\Psi m$ changes and respiratory suppression (Yadava and Nicholls, 2007).

CONCLUSIONS

In summary, our experiments in astrocyte-enriched cultures showed that DJ-1 knock-down significantly reduced mitochondrial motility in cellular processes, but had minimal effects on mitochondrial fission or fusion. However, the astrocyte mitochondrial dynamics findings were quite different in neuron–astrocyte contact co-cultures. Here, the astrocyte process motility results were less robust, whereas the astrocyte cell body mitochondrial fusion rates were (i) baseline and equal in both the untreated DJ-1 knock-down and control astrocytes, (ii) significantly reduced in DJ-1 knock-down versus control astrocytes after treatment with 20 nM rotenone, and (iii) suppressed and equal in both the DJ-1 knock-down and control astrocytes after treatment with 40 nM rotenone. Because these results closely parallel our previous neuronal viability data in the same co-culture system, it is possible that they are relevant to the mechanism of DJ-1 modulated, astrocyte-mediated neuroprotection against rotenone. These data, combined with our finding that DJ-1 knock-down enhanced rotenone-induced suppression of the astrocyte $\Delta\Psi m$, support the conclusion that DJ-1 deficiency impairs astrocyte mitochondrial physiology on multiple levels. Our studies also show that astrocyte mitochondrial behavior differs between sub-cellular regions and that it can be affected by the physical presence of neurons.

Supplementary Material

Refer to Web version on PubMed Central for supplementary material.

Acknowledgments

We thank Bethann Gabris for technical assistance. We thank Steve Cassady and Victor Van Laar for technical and analytical software assistance. This work was supported by departmental funds to D.A.H.

Abbreviations

ABAM	antibiotic-antimycotic
CS	calf serum
DIV	days *in vitro*
DMEM	Dulbecco's modified Eagle media
DMSO	dimethyl sulfoxide
ECAR	extracellular acidification rate
FCCP	p-trifluoromethoxy carbonyl cyanide phenyl hydrazone
FCS	fetal calf serum
GFAP	glial fibrillary acidic protein
HEPES	4-(2-hydroxyethyl)-1-piperazineethane-sulfonic acid
JC-1	5,5′,6,6′-tetrachloro-1,1′,3,3′-tetraethylbenzimida-zolyl-carbocyanine iodide
MPTP	1-methyl-4-phenyl-1,2,3,6-tetrahydro-pyridine
mtDNA	mitochondrial deoxyribonucleic acid
mtDsRed2	mitochondria-targeted red fluorescent protein
mtPAGFP	mitochondria-targeted photoactivatable green fluorescent protein
OCR	oxygen consumption rate
PINK1	phosphate and tensin homolog [PTEN] induced putative kinase 1
PD	Parkinson's disease
ROI	region of interest
ROS	reactive oxygen species
siDJ#2	anti-mouse DJ-1 siRNA
siNS	non-silencing siRNA
siRNA	small interfering ribonucleic acid
ΔΨm	mitochondrial membrane potential

References

Aleyasin H, Rousseaux MW, Phillips M, Kim RH, Bland RJ, Callaghan S, Slack RS, During MJ, Mak TW, Park DS. The Parkinson's disease gene DJ-1 is also a key regulator of stroke-induced damage. Proc Natl Acad Sci U S A. 2007; 104:18748–18753. [PubMed: 18003894]

Arnold B, Cassady SJ, VanLaar VS, Berman SB. Integrating multiple aspects of mitochondrial dynamics in neurons: age-related differences and dynamic changes in a chronic rotenone model. Neurobiol Dis. 2011; 41:189–200. [PubMed: 20850532]

Ascherio A, Chen H, Weisskopf MG, O'Reilly E, McCullough ML, Calle EE, Schwarzschild MA, Thun MJ. Pesticide exposure and risk for Parkinson's disease. Ann Neurol. 2006; 60:197–203. [PubMed: 16802290]

Ashley AK, Hanneman WH, Katoh T, Moreno JA, Pollack A, Tjalkens RB, Legare ME. Analysis of targeted mutation in DJ-1 on cellular function in primary astrocytes. Toxicol Lett. 2009; 184:186–191. [PubMed: 19063952]

Ballard PA, Tetrud JW, Langston JW. Permanent human parkinsonism due to 1-methyl-4-phenyl-1,2,3,6-tetrahydropyridine (MPTP): seven cases. Neurology. 1985; 35:949–956. [PubMed: 3874373]

Barsoum MJ, Yuan H, Gerencser AA, Liot G, Kushnareva Y, Gräber S, Kovacs I, Lee WD, Waggoner J, Cui J, White AD, Bossy B, Martinou JC, Youle RJ, Lipton SA, Ellisman MH, Perkins GA, Bossy-Wetzel E. Nitric oxide-induced mitochondrial fission is regulated by dynamin-related GTPases in neurons. EMBO J. 2006; 25:3900–3911. [PubMed: 16874299]

Benard G, Bellance N, James D, Parrone P, Fernandez H, Letellier T, Rossignol R. Mitochondrial bioenergetics and structural network organization. J Cell Sci. 2007; 120:838– 848. [PubMed: 17298981]

Berman SB, Chen YB, Qi B, McCaffery JM, Rucker EB 3rd, Goebbels S, Nave KA, Arnold BA, Jonas EA, Pineda FJ, Hardwick JM. Bcl-x L increases mitochondrial fission, fusion, and biomass in neurons. J Cell Biol. 2009; 184:707–719. [PubMed: 19255249]

Betarbet R, Sherer TB, MacKenzie G, Garcia-Osuna M, Panov AV, Greenamyre JT. Chronic systemic pesticide exposure reproduces features of Parkinson's disease. Nat Neurosci. 2000; 3:1301–1306. [PubMed: 11100151]

Blackinton J, Lakshminarasimhan M, Thomas KJ, Ahmad R, Greggio E, Raza AS, Cookson MR, Wilson MA. Formation of a stabilized cysteine sulfinic acid is critical for the mitochondrial function of the parkinsonism protein DJ-1. J Biol Chem. 2009; 284:6476– 6485. [PubMed: 19124468]

Blin O, Desnuelle C, Rascol O, Borg M, Peyro Saint Paul H, Azulay JP, Billé F, Figarella D, Coulom F, Pellissier JF, et al. Mitochondrial respiratory failure in skeletal muscle from patients with Parkinson's disease and multiple system atrophy. J Neurol Sci. 1994; 125:95–101. [PubMed: 7964895]

Bonifati V, Rizzu P, van Baren MJ, Schaap O, Breedveld GJ, Krieger E, Dekker MC, Squitieri F, Ibanez P, Joosse M, van Dongen JW, Vanacore N, van Swieten JC, Brice A, Meco G, van Duijn CM, Oostra BA, Heutink P. Mutations in the DJ-1 gene associated with autosomal recessive early-onset parkinsonism. Science. 2003; 299:256–259. [PubMed: 12446870]

Borland MK, Trimmer PA, Rubinstein JD, Keeney PM, Mohanakumar K, Liu L, Bennett JP Jr. Chronic, low-dose rotenone reproduces Lewy neurites found in early stages of Parkinson's disease, reduces mitochondrial movement and slowly kills differentiated SH-SY5Y neural cells. Mol Neurodegener. 2008; 3:21. [PubMed: 19114014]

Brown TP, Rumsby PC, Capleton AC, Rushton L, Levy LS. Pesticides and Parkinson's disease—is there a link? Environ Health Perspect. 2006; 114:156–164. [PubMed: 16451848]

Büeler H. Impaired mitochondrial dynamics and function in the pathogenesis of Parkinson's disease. Exp Neurol. 2009; 218:235–246. [PubMed: 19303005]

Burbulla LF, Krebiehl G, Krüger R. Balance is the challenge—the impact of mitochondrial dynamics in Parkinson's disease. Eur J Clin Invest. 2010; 40:1048–1060. [PubMed: 20735469]

Canet-Avilés RM, Wilson MA, Miller DW, Ahmad R, McLendon C, Bandyopadhyay S, Baptista MJ, Ringe D, Petsko GA, Cookson MR. The Parkinson's disease protein DJ-1 is neuroprotective due to cysteine-sulfinic acid-driven mitochondrial localization. Proc Natl Acad Sci U S A. 2004; 101:9103–9108. [PubMed: 15181200]

Cannon JR, Tapias V, Na HM, Honick AS, Drolet RE, Greenamyre JT. A highly reproducible rotenone model of Parkinson's disease. Neurobiol Dis. 2009; 34:279–290. [PubMed: 19385059]

Clements CM, McNally RS, Conti BJ, Mak TW, Ting JP. DJ-1, a cancer- and Parkinson's disease-associated protein, stabilizes the antioxidant transcriptional master regulator Nrf2. Proc Natl Acad Sci U S A. 2006; 103:15091–15096. [PubMed: 17015834]

Cooper JM, Mann VM, Krige D, Schapira AH. Human mitochondrial complex I dysfunction. Biochim Biophys Acta. 1992; 1101:198–203. [PubMed: 1633185]

Esteves AR, Lu J, Rodova M, Onyango I, Lezi E, Dubinsky R, Lyons KE, Pahwa R, Burns JM, Cardoso SM, Swerdlow RH. Mitochondrial respiration and respiration-associated proteins in cell lines created through Parkinson's subject mitochondrial transfer. J Neurochem. 2010; 113:674–682. [PubMed: 20132468]

Feng J. Microtubule: a common target for parkin and Parkinson's disease toxins. Neuroscientist. 2006; 12:469– 476. [PubMed: 17079513]

Ferrick DA, Neilson A, Beeson C. Advances in measuring cellular bioenergetics using extracellular flux. Drug Discov Today. 2008; 13:268–274. [PubMed: 18342804]

Gash DM, Rutland K, Hudson NL, Sullivan PG, Bing G, Cass WA, Pandya JD, Liu M, Choi DY, Hunter RL, Gerhardt GA, Smith CD, Slevin JT, Prince TS. Trichloroethylene: Parkinsonism and complex 1 mitochondrial neurotoxicity. Ann Neurol. 2008; 63:184–192. [PubMed: 18157908]

Gerencser AA, Neilson A, Choi SW, Edman U, Yadava N, Oh RJ, Ferrick DA, Nicholls DG, Brand MD. Quantitative microplate-based respirometry with correction for oxygen diffusion. Anal Chem. 2009; 81:6868– 6878. [PubMed: 19555051]

Haas RH, Nasirian F, Nakano K, Ward D, Pay M, Hill R, Shults CW. Low platelet mitochondrial complex I and complex II/III activity in early untreated Parkinson's disease. Ann Neurol. 1995; 37:714–722. [PubMed: 7778844]

Hao LY, Giasson BI, Bonini NM. DJ-1 is critical for mitochondrial function and rescues PINK1 loss of function. Proc Natl Acad Sci U S A. 2010; 107:9747–9752. [PubMed: 20457924]

Heggeness MH, Simon M, Singer SJ. Association of mitochondria with microtubules in cultured cells. Proc Natl Acad Sci U S A. 1978; 75:3863–3866. [PubMed: 80800]

Hollenbeck PJ, Saxton WM. The axonal transport of mitochondria. J Cell Sci. 2005; 118:5411–5419. [PubMed: 16306220]

Irrcher I, Aleyasin H, Seifert EL, Hewitt SJ, Chhabra S, Phillips M, Lutz AK, Rousseaux MW, Bevilacqua L, Jahani-Asl A, Callaghan S, MacLaurin JG, Winklhofer KF, Rizzu P, Rippstein P, Kim RH, Chen CX, Fon EA, Slack RS, Harper ME, McBride HM, Mak TW, Park DS. Loss of the Parkinson's disease-linked gene DJ-1 perturbs mitochondrial dynamics. Hum Mol Genet. 2010; 19:3734–3746. [PubMed: 20639397]

Junn E, Taniguchi H, Jeong BS, Zhao X, Ichijo H, Mouradian MM. Interaction of DJ-1 with Daxx inhibits apoptosis signal-regulating kinase 1 activity and cell death. Proc Natl Acad Sci U S A. 2005; 102:9691–9696. [PubMed: 15983381]

Kamp F, Exner N, Lutz AK, Wender N, Hegermann J, Brunner B, Nuscher B, Bartels T, Giese A, Beyer K, Eimer S, Winklhofer KF, Haass C. Inhibition of mitochondrial fusion by alpha-synuclein is rescued by PINK1, Parkin and DJ-1. EMBO J. 2010; 29:3571–3589. [PubMed: 20842103]

Kim YJ, Ko HH, Han ES, Lee CS. Lamotrigine inhibition of rotenone- or 1-methyl-4-phenylpyridinium-induced mitochondrial damage and cell death. Brain Res Bull. 2007; 71:633–640. [PubMed: 17292807]

Kitada T, Asakawa S, Hattori N, Matsumine H, Yamamura Y, Minoshima S, Yokochi M, Mizuno Y, Shimizu N. Mutations in the parkin gene cause autosomal recessive juvenile parkinsonism. Nature. 1998; 392:605– 608. [PubMed: 9560156]

Knott AB, Bossy-Wetzel E. Impairing the mitochondrial fission and fusion balance: a new mechanism of neurodegeneration. Ann N Y Acad Sci. 2008; 1147:283–292. [PubMed: 19076450]

Koopman WJ, Hink MA, Verkaart S, Visch HJ, Smeitink JA, Willems PH. Partial complex I inhibition decreases mitochondrial motility and increases matrix protein diffusion as revealed by fluorescence correlation spectroscopy. Biochim Biophys Acta. 2007; 1767:940–947. [PubMed: 17490603]

Krebiehl G, Ruckerbauer S, Burbulla LF, Kieper N, Maurer B, Waak J, Wolburg H, Gizatullina Z, Gellerich FN, Woitalla D, Riess O, Kahle PJ, Proikas-Cezanne T, Krüger R. Reduced basal

autophagy and impaired mitochondrial dynamics due to loss of Parkinson's disease-associated protein DJ-1. PLoS One. 2010; 5:e9367. [PubMed: 20186336]

Langston JW, Forno LS, Rebert CS, Irwin I. Selective nigral toxicity after systemic administration of 1-methyl-4-phenyl-1,2,5,6-tetrahydropyrine (MPTP) in the squirrel monkey. Brain Res. 1984; 292:390–394. [PubMed: 6607092]

Li Z, Okamoto K, Hayashi Y, Sheng M. The importance of dendritic mitochondria in the morphogenesis and plasticity of spines and synapses. Cell. 2004; 119:873– 887. [PubMed: 15607982]

Liu F, Nguyen JL, Hulleman JD, Li L, Rochet JC. Mechanisms of DJ-1 neuroprotection in a cellular model of Parkinson's disease. J Neurochem. 2008; 105:2435–2453. [PubMed: 18331584]

Mortiboys H, Thomas KJ, Koopman WJ, Klaffke S, Abou-Sleiman P, Olpin S, Wood NW, Willems PH, Smeitink JA, Cookson MR, Bandmann O. Mitochondrial function and morphology are impaired in parkin-mutant fibroblasts. Ann Neurol. 2008; 64:555–565. [PubMed: 19067348]

Mullett SJ, Hamilton RL, Hinkle DA. DJ-1 immunoreactivity in human brain astrocytes is dependent on infarct presence and infarct age. Neuropathology. 2009; 29:125–131. [PubMed: 18647263]

Mullett SJ, Hinkle DA. DJ-1 knock-down in astrocytes impairs astrocyte-mediated neuroprotection against rotenone. Neurobiol Dis. 2009; 33:28–36. [PubMed: 18930142]

Mullett SJ, Hinkle DA. DJ-1 deficiency in astrocytes selectively enhances mitochondrial complex I inhibitor-induced neurotoxicity. J Neurochem. 2011; 117:375–387. [PubMed: 21219333]

Oberheim NA, Takano T, Han X, He W, Lin JH, Wang F, Xu Q, Wyatt JD, Pilcher W, Ojemann JG, Ransom BR, Goldman SA, Nedergaard M. Uniquely hominid features of adult human astrocytes. J Neurosci. 2009; 29:3276–3287. [PubMed: 19279265]

Oberheim NA, Wang X, Goldman S, Nedergaard M. Astrocytic complexity distinguishes the human brain. Trends Neurosci. 2006; 29:547–553. [PubMed: 16938356]

Okamoto K, Shaw JM. Mitochondrial morphology and dynamics in yeast and multicellular eukaryotes. Annu Rev Genet. 2005; 39:503–536. [PubMed: 16285870]

Ouyang YB, Giffard RG. Changes in astrocyte mitochondrial function with stress: effects of Bcl-2 family proteins. Neurochem Int. 2004; 45:371–379. [PubMed: 15145551]

Paisén-Ruíz C, Jain S, Evans EW, Gilks WP, Simón J, van der Brug M, López de Munain A, Aparicio S, Gil AM, Khan N, Johnson J, Martinez JR, Nicholl D, Carrera IM, Pena AS, de Silva R, Lees A, Martí-Massó JF, Pérez-Tur J, Wood NW, Singleton AB. Cloning of the gene containing mutations that cause PARK8-linked Parkinson's disease. Neuron. 2004; 44:595– 600. [PubMed: 15541308]

Panov A, Dikalov S, Shalbuyeva N, Taylor G, Sherer T, Greenamyre JT. Rotenone model of Parkinson disease: multiple brain mitochondria dysfunctions after short term systemic rotenone intoxication. J Biol Chem. 2005; 280:42026– 42035. [PubMed: 16243845]

Parker WD Jr, Parks JK, Swerdlow RH. Complex I deficiency in Parkinson's disease frontal cortex. Brain Res. 2008; 1189:215–218. [PubMed: 18061150]

Pham NA, Richardson T, Cameron J, Chue B, Robinson BH. Altered mitochondrial structure and motion dynamics in living cells with energy metabolism defects revealed by real time microscope imaging. Microsc Microanal. 2004; 10:247–260. [PubMed: 15306050]

Radad K, Rausch WD, Gille G. Rotenone induces cell death in primary dopaminergic culture by increasing ROS production and inhibiting mitochondrial respiration. Neurochem Int. 2006; 49:379–386. [PubMed: 16580092]

Reers M, Smiley ST, Mottola-Hartshorn C, Chen A, Lin M, Chen LB. Mitochondrial membrane potential monitored by JC-1 dye. Methods Enzymol. 1995; 260:406– 417. [PubMed: 8592463]

Reers M, Smith TW, Chen LB. J-aggregate formation of a carbocyanine as a quantitative fluorescent indicator of membrane potential. Biochemistry. 1991; 30:4480– 4486. [PubMed: 2021638]

Rizzu P, Hinkle DA, Zhukareva V, Bonifati V, Severijnen LA, Martinez D, Ravid R, Kamphorst W, Eberwine JH, Lee VM, Trojanowski JQ, Heutink P. DJ-1 colocalizes with tau inclusions: a link between parkinsonism and dementia. Ann Neurol. 2004; 55:113–118. [PubMed: 14705119]

Sanchez M, Gastaldi L, Remedi M, Céceres A, Landa C. Rotenone-induced toxicity is mediated by Rho-GTPases in hippocampal neurons. Toxicol Sci. 2008; 104:352–361. [PubMed: 18480073]

Sbalzarini IF, Koumoutsakos P. Feature point tracking and trajectory analysis for video imaging in cell biology. J Struct Biol. 2005; 151:182–195. [PubMed: 16043363]

Schapira AH. Disease modification in Parkinson's disease. Lancet Neurol. 2004; 3:362–368. [PubMed: 15157851]

Schapira AH, Cooper JM, Dexter D, Clark JB, Jenner P, Marsden CD. Mitochondrial complex I deficiency in Parkinson's disease. J Neurochem. 1990; 54:823– 827. [PubMed: 2154550]

Sherer TB, Richardson JR, Testa CM, Seo BB, Panov AV, Yagi T, Matsuno-Yagi A, Miller GW, Greenamyre JT. Mechanism of toxicity of pesticides acting at complex I: relevance to environmental etiologies of Parkinson's disease. J Neurochem. 2007; 100:1469–1479. [PubMed: 17241123]

Smiley ST, Reers M, Mottola-Hartshorn C, Lin M, Chen A, Smith TW, Steele GD Jr, Chen LB. Intracellular heterogeneity in mitochondrial membrane potentials revealed by a J-aggregate-forming lipophilic cation JC-1. Proc Natl Acad Sci U S A. 1991; 88:3671–3675. [PubMed: 2023917]

Taira T, Saito Y, Niki T, Iguchi-Ariga SM, Takahashi K, Ariga H. DJ-1 has a role in antioxidative stress to prevent cell death. EMBO Rep. 2004; 5:213–218. [PubMed: 14749723]

Tanner, CM.; Kamel, F.; Ross, GW.; Hoppin, JA.; Goldman, SM.; Korrell, M.; Marras, C.; Bhudhikanok, GS.; Kasten, M.; Chade, A.; Comyns, K.; Meng, C.; Priestley, B.; Fernandez, HH.; Cambi, F.; Umbach, DM.; Blair, A.; Sandler, DP.; Langston, JW. Rotenone, paraquat, and Parkinson's disease. American Neurological Association; 2010. Abstract 350182

Thomas KJ, McCoy MK, Blackinton J, Beilina A, van der Brug M, Sandebring A, Miller D, Maric D, Cedazo-Minguez A, Cookson MR. DJ-1 acts in parallel to the PINK1/parkin pathway to control mitochondrial function and autophagy. Hum Mol Genet. 2011; 20:40–50. [PubMed: 20940149]

Trimmer PA, Bennett JP Jr. The cybrid model of sporadic Parkinson's disease. Exp Neurol. 2009; 218:320–325. [PubMed: 19328199]

Van Laar VS, Berman SB. Mitochondrial dynamics in Parkinson's disease. Exp Neurol. 2009; 218:247–256. [PubMed: 19332061]

Ved R, Saha S, Westlund B, Perier C, Burnam L, Sluder A, Hoener M, Rodrigues CM, Alfonso A, Steer C, Liu L, Przedborski S, Wolozin B. Similar patterns of mitochondrial vulnerability and rescue induced by genetic modification of alpha-synuclein, parkin, and DJ-1 in Caenorhabditis elegans. J Biol Chem. 2005; 280:42655– 42668. [PubMed: 16239214]

Volterra A, Meldolesi J. Astrocytes, from brain glue to communication elements: the revolution continues. Nat Rev Neurosci. 2005; 6:626– 640. [PubMed: 16025096]

Westermann B. Merging mitochondria matters: cellular role and molecular machinery of mitochondrial fusion. EMBO Rep. 2002; 3:527–531. [PubMed: 12052774]

White RJ, Reynolds IJ. Mitochondrial depolarization in glutamate-stimulated neurons: an early signal specific to excitotoxin exposure. J Neurosci. 1996; 16:5688–5697. [PubMed: 8795624]

Winklhofer KF, Haass C. Mitochondrial dysfunction in Parkinson's disease. Biochim Biophys Acta. 2010; 1802:29– 44. [PubMed: 19733240]

Xu J, Zhong N, Wang H, Elias JE, Kim CY, Woldman I, Pifl C, Gygi SP, Geula C, Yankner BA. The Parkinson's disease-associated DJ-1 protein is a transcriptional co-activator that protects against neuronal apoptosis. Hum Mol Genet. 2005; 14:1231–1241. [PubMed: 15790595]

Yadava N, Nicholls DG. Spare respiratory capacity rather than oxidative stress regulates glutamate excitotoxicity after partial respiratory inhibition of mitochondrial complex I with rotenone. J Neurosci. 2007; 27:7310–7317. [PubMed: 17611283]

Zhou W, Freed CR. DJ-1 up-regulates glutathione synthesis during oxidative stress and inhibits A53T alpha-synuclein toxicity. J Biol Chem. 2005; 280:43150– 43158. [PubMed: 16227205]

Zhu J, Chu CT. Mitochondrial dysfunction in Parkinson's disease. J Alzheimers Dis. 2010; 20 (Suppl 2):S325–S334. [PubMed: 20442495]

APPENDIX

Supplementary data

Supplementary data associated with this article can be found, in the online version, at doi: 10.1016/j.neuroscience.2011.08.016.

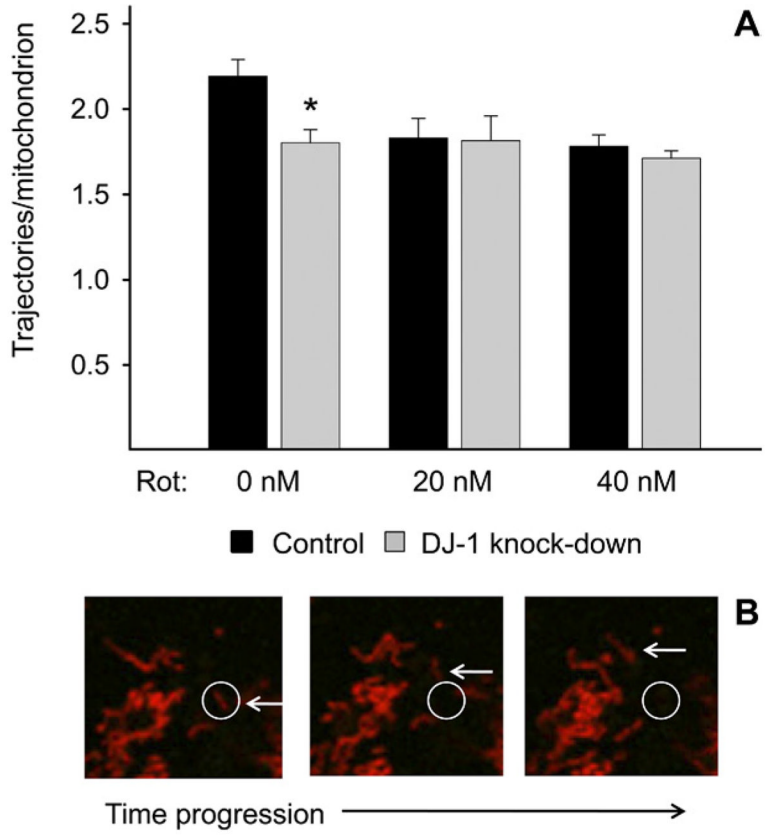

Fig. 1.

Whole-cell mitochondrial motility was impaired by DJ-1 knockdown in astrocyte-enriched cultures. Control (black bars) and DJ-1 knock-down (gray bars) astrocytes were transfected with mtDsRed2 to identify and track live mitochondria, and then treated for 24 h with 0, 20, or 40 nM rotenone. (A) Untreated DJ-1 knock-down astrocytes exhibited reduced mitochondrial motility (trajectories beyond a radius threshold/mitochondrion) relative to control astrocytes, but rotenone treatments did not augment this effect. Asterisks (*) represent $P<0.05$ for same-treatment comparisons between control and DJ-1 knockdown astrocytes by paired *t*-tests. Mean±SE shown, $n=6$. (B) Sequential photomicrograph frames of a mobile mtDsRed2+ mitochondrion moving beyond a simulated radius threshold. For interpretation of the references to color in this figure legend, the reader is referred to the Web version of this article.

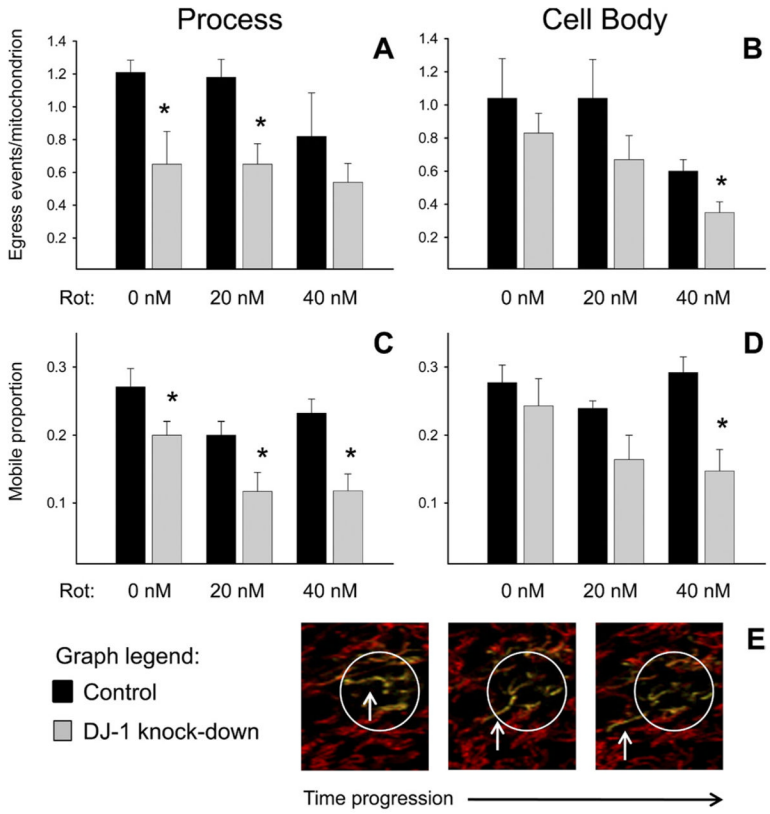

Fig. 2.

DJ-1 knock-down reduced mitochondrial motility predominantly at cellular processes in astrocyte-enriched cultures. Control (black bars) and DJ-1 knock-down (gray bars) astrocytes were co-transfected with mtDsRed2 and mtPAGFP, and then treated for 24 h with 0, 20, or 40 nM rotenone. Mitochondrial egress events (mitochondrial movements across an ROI boundary, (A–B)) and mobile mitochondria (within an ROI, (C–D)) were counted and then normalized to the total number of mitochondria within the same ROI. Asterisks (*) represent $P<0.05$ for same-treatment comparisons between control and DJ-1 knock-down astrocytes by paired *t*-tests. Mean±SE shown, $n=6$. (A) In astrocyte processes, DJ-1 knock-down reduced mitochondrial egress in untreated and 20 nM rotenone treated cells. (B) In astrocyte cell bodies, DJ-1 knock-down caused a trend towards reduced mitochondrial egress that was not significant until the cells were treated with 40 nM rotenone. (C) In astrocyte processes, DJ-1 knock-down reduced the mitochondrial mobile proportion under all conditions of treatment. (D) In astrocyte cell bodies, DJ-1 knock-down caused a trend towards reduced mitochondrial mobile proportion that was not significant until the cells were treated with 40 nM rotenone. (E) Sequential photomicrograph frames of a mobile photoactivated mtPAGFP+ (green fluorescent) mitochondrion that leaves a simulated laser-photoactivated ROI. For interpretation of the references to color in this figure legend, the reader is referred to the Web version of this article.

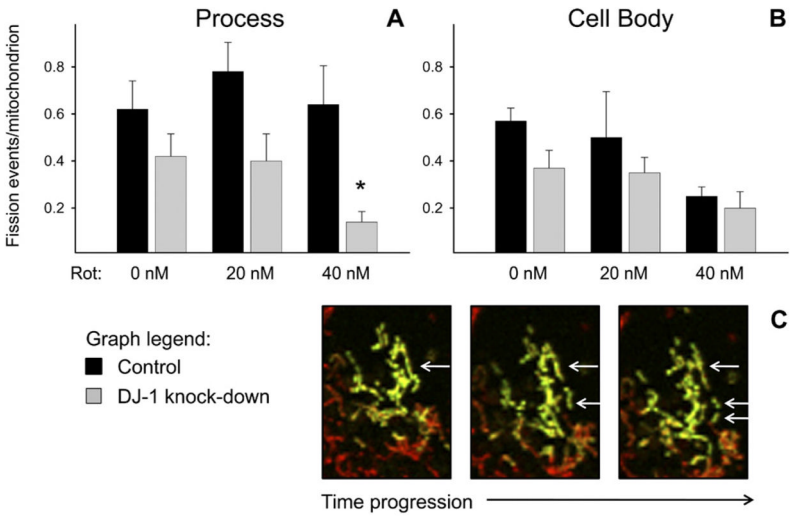

Fig. 3.

DJ-1 knock-down reduced mitochondrial fission in cellular processes only in the presence of high-dose rotenone in astrocyte-enriched cultures. Control (black bars) and DJ-1 knock-down (gray bars) astrocytes were co-transfected with mtDsRed2 and mtPAGFP, and then treated for 24 h with 0, 20, or 40 nM rotenone. Mitochondrial fission events (fragmentation of mtPAGFP+ mitochondria into separate organelles) were counted and normalized to the total number of mitochondria within the ROI. Asterisks (*) represent $P<0.05$ for same-treatment comparisons between control and DJ-1 knock-down astrocytes by paired *t*-tests. Mean±SE shown, $n=6$. (A) In astrocyte processes, DJ-1 knock-down caused a trend towards reduced mitochondrial fission that was only significant after treatment with 40 nM rotenone. (B) In astrocyte cell bodies, DJ-1 knock-down did not alter mitochondrial fission. (C) Sequential photomicrograph frames of an mtPAGFP+ (green fluorescent) mitochondrion that underwent two fission events within the laser-photoactivated ROI. For interpretation of the references to color in this figure legend, the reader is referred to the Web version of this article.

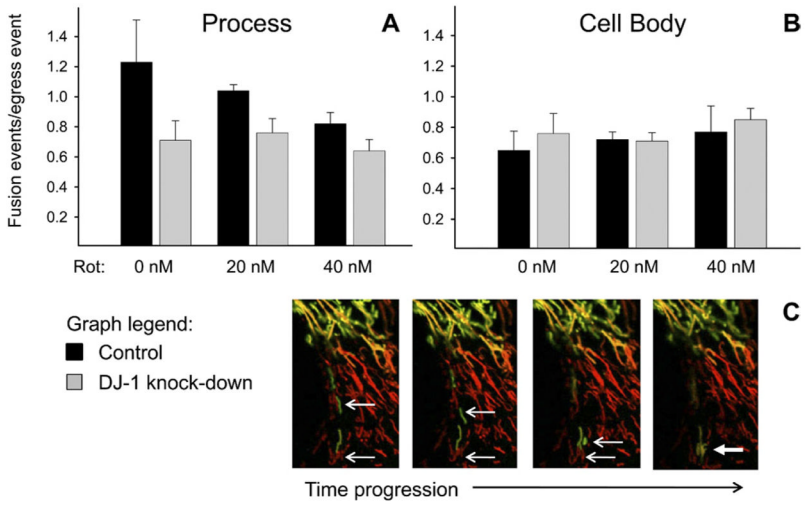

Fig. 4.

DJ-1 knock-down did not alter mitochondrial fusion in astrocyte-enriched cultures. Control (black bars) and DJ-1 knock-down (gray bars) astrocytes were co-transfected with mtDsRed2 and mtPAGFP, and then treated for 24 h with 0, 20, or 40 nM rotenone. Mitochondrial fusion events (mixing of adjacent organelle mtPAGFP+ and mtDsRed2+ mitochondrial contents) were counted and normalized to the total number of mitochondrial egress events from that ROI. Same-treatment comparisons were made between control and DJ-1 knock-down astrocytes by paired *t*-tests. Mean±SE shown, n=6. (A) In astrocyte processes, neither DJ-1 knock-down nor rotenone treatment altered mitochondrial fusion. (B) The same was true in astrocyte cell bodies. (C) Sequential photomicrograph frames showing a fusion event between an mtPAGFP+ (green) mitochondrion and an mtDsRed2+ (red) mitochondrion. For interpretation of the references to color in this figure legend, the reader is referred to the Web version of this article.

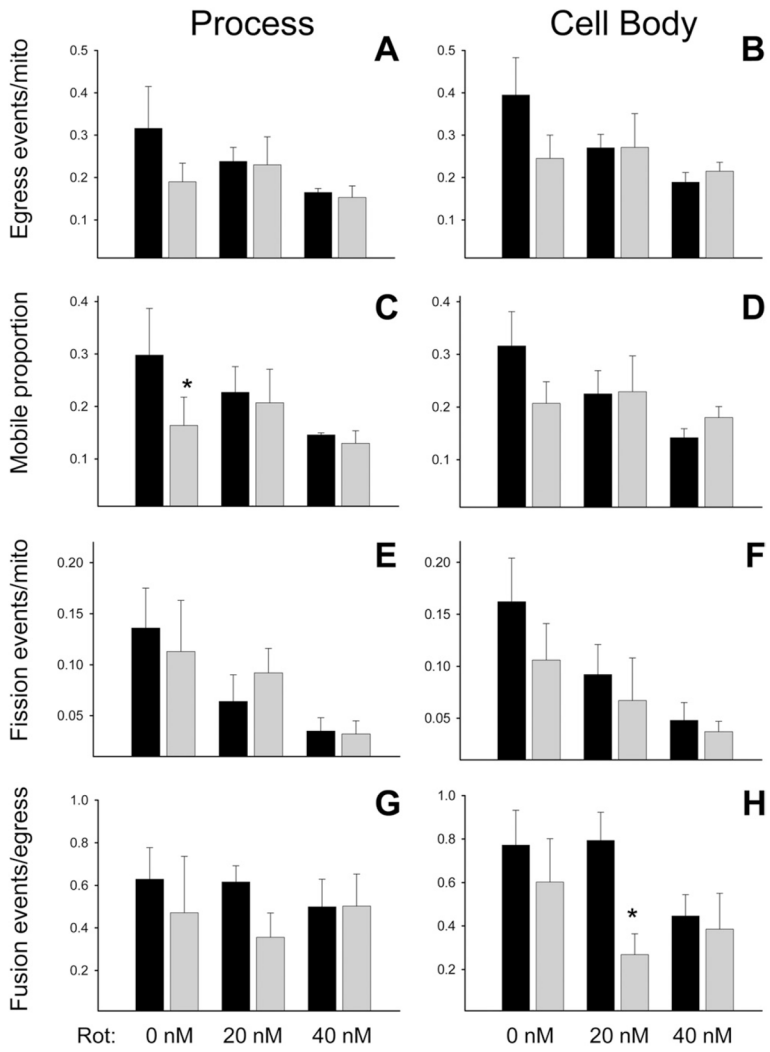

Fig. 5.

In the presence of contact co-cultured neurons, astrocytic DJ-1 knock-down reduced mitochondrial motility in untreated astrocyte processes and mitochondrial fusion in rotenone-treated astrocyte cell bodies. Control (black bars) and DJ-1 knock-down (gray bars) astrocytes were co-transfected with mtDsRed2 and mtPAGFP, and then treated for 24 h with 0, 20, or 40 nM rotenone. Astrocyte mitochondrial egress events (A–B), mobile proportions (C–D), fission events (E–F), and fusion events (G–H) were calculated in cellular processes (A, C, E, G) and cell bodies (B, D, F, H). Asterisks (*) represent $P<0.05$ for same-treatment comparisons made between control and DJ-1 knock-down astrocytes by paired *t*-tests. Mean±SE shown, $n=6$. (A) In astrocyte processes, DJ-1 knock-down caused a trend towards reduced mitochondrial egress only in untreated cells. (B) In astrocyte cell bodies, a similar pattern was seen. (C) In astrocyte processes, DJ-1 knock-down reduced the mitochondrial mobile proportion only in untreated cells. (D–G) DJ-1 knock-down did not affect the mitochondrial mobile proportion in astrocyte cell bodies (D), mitochondrial fission in astrocyte processes (E) or cell bodies (F), or mitochondrial fusion in astrocyte processes (G). (H) In astrocyte cell bodies, DJ-1 knock-down reduced mitochondrial fusion in cells treated with 20 nM rotenone, but the effect at 40 nM was obscured by a similar reduction in fusion induced by rotenone.

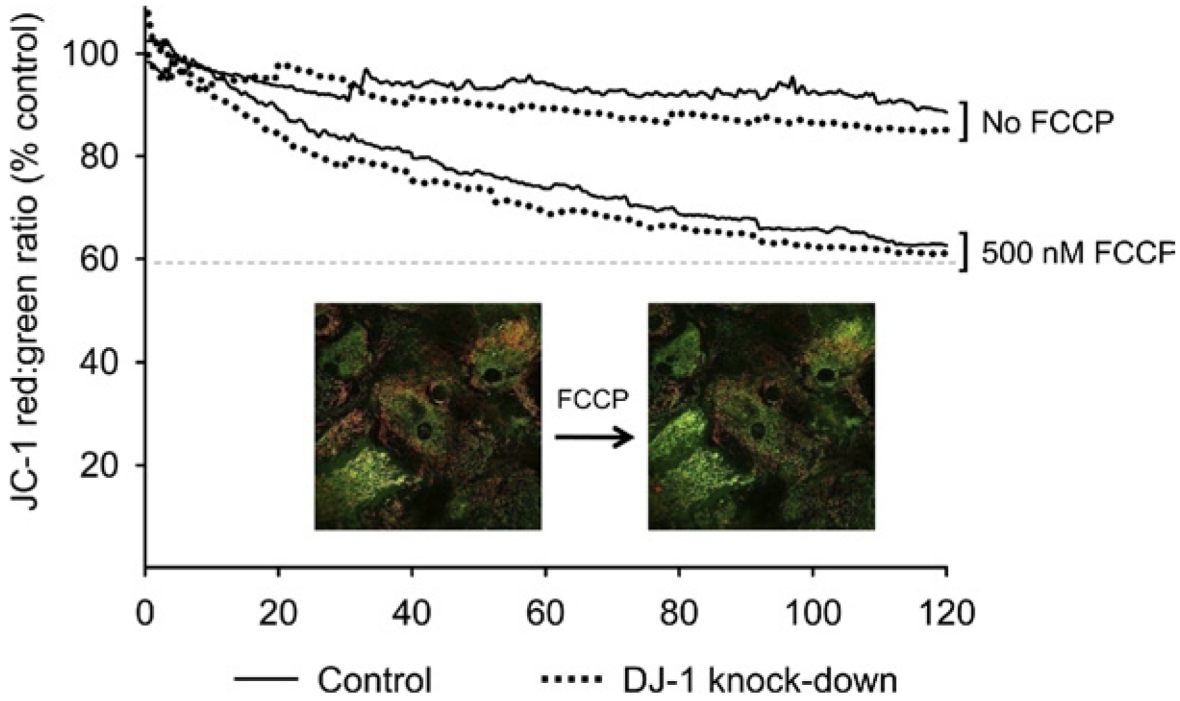

Fig. 6.

DJ-1 knock-down did not alter the baseline ΔΨm or enhance FCCP-induced ΔΨm depolarization in astrocyte-enriched cultures. Astrocytes in the field of view were imaged every 30 s over 2 h to determine the JC-1 red:green emission ratio (times are shown in minutes on the x-axis). A red-to-green shift, or reduced ratio, represented depolarized ΔΨm (see photomicrograph insert). Untreated astrocytes displayed a small reduction in red:green fluorescence as a function of time, but there was no significant difference between control (solid lines) and DJ-1 knock-down (dashed lines) cells. 500 nM FCCP reduced the red:green ratio more robustly, but there was again no significant difference in ΔΨm between the control and DJ-1 knockdown astrocytes. Maximal ΔΨm depolarization occurred by ~90 m (the 60% asymptote line). For interpretation of the references to color in this figure legend, the reader is referred to the Web version of this article.

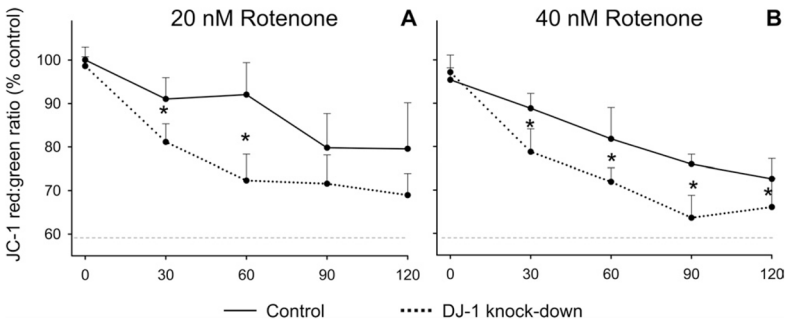

Fig. 7.

DJ-1 knock-down enhanced rotenone-induced ΔΨm depolarization in astrocyte-enriched cultures. Control (solid lines) and DJ-1 knock-down (dashed lines) astrocytes were treated with 20 or 40 nM rotenone and imaged every 30 s for 2 h using a confocal microscope to determine the JC-1 dye red:green emission ratio (times are shown in minutes on the x-axis). An emission shift from red to green (reduced ratio) represented a depolarization in ΔΨm. Asterisks (*) represent $P<0.05$ for same-time/treatment comparisons between control and DJ-1 knock-down astrocytes by paired *t*-tests. Mean±SE shown, $n=6$. (A) DJ-1 knock-down significantly enhanced the 20 nM rotenone-induced reduction in red:green emission at 30 and 60 m. A similar trend persisted at 90 and 120 m. (B) DJ-1 knock-down significantly enhanced the 40 nM rotenone-induced reduction in red:green emission at all time points after toxin administration.

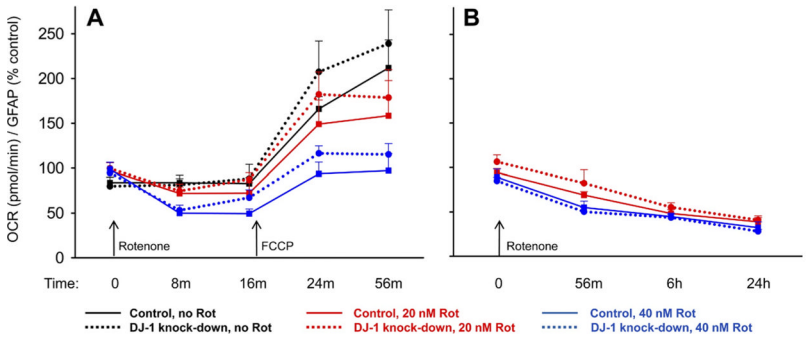

Fig. 8.

DJ-1 knock-down did not reduce oxygen consumption rates (OCR) in astrocyte-enriched cultures. Mitochondrial respiration was analyzed by measuring OCR in living astrocytes using a Seahorse XF24 analyzer. The OCR values were then normalized to total astrocyte numbers, as assessed by GFAP in-cell Western analysis, on the same plates. Control (solid lines) and DJ-1 knock-down (dashed lines) astrocytes were compared at baseline, after treatments with 0, 20, or 40 nM rotenone (A, B), and then after the addition of 500 nM FCCP (A). In each graph, same-time/treatment comparisons were made between control and DJ-1 knock-down astrocytes by paired *t*-tests. Mean±SE shown, $n=5$. (A) There was no difference between the OCR of control and DJ-1 knock-down astrocytes under any treatment condition over a 1 h period. However, as expected, rotenone treatment reduced the OCR, FCCP stimulated the OCR, and rotenone reduced the FCCP-induced stimulation. The data in this graph are expressed as percent control relative to OCR/GFAP values from same-time no rotenone/no FCCP control wells on the same plates. (B) Extended assessments over 24 h did not show any significant differences between the OCR of control and DJ-1 knock-down astrocytes, but did show the expected rotenone-induced reduction in OCR. The data in this graph are expressed as percent control relative to OCR/GFAP values from same-time no rotenone control wells on the same plates. For interpretation of the references to color in this figure legend, the reader is referred to the Web version of this article.

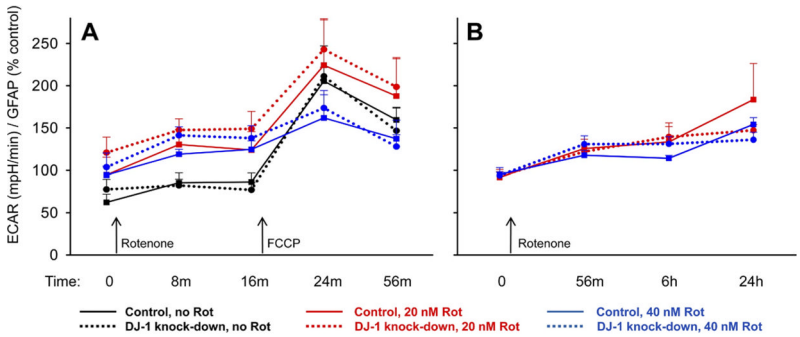

Fig. 9.

DJ-1 knock-down did not enhance extracellular acidification rates (ECAR) in astrocyte-enriched cultures. Mitochondrial glycolytic flux was analyzed by measuring ECAR in living astrocytes using a Seahorse XF24 analyzer. The ECAR values were then normalized to total astrocyte numbers, as assessed by GFAP in-cell Western analysis, on the same plates. Control (solid lines) and DJ-1 knock-down (dashed lines) astrocytes were compared at baseline, after treatments with 0, 20, or 40 nM rotenone (A, B), and then after the addition of 500 nM FCCP (A). In each graph, same-time/treatment comparisons were made between control and DJ-1 knock-down astrocytes by paired *t*-tests. Mean±SE shown, n=5. (A) There was no difference between the ECAR of control and DJ-1 knock-down astrocytes under any treatment condition over a 1 h period. However, as expected, FCCP (and, to a lesser extent, rotenone) stimulated the ECAR. The data in this graph are expressed as percent control relative to ECAR/GFAP values from same-time no rotenone/no FCCP control wells on the same plates. (B) Extended assessments over 24 h did not show any significant differences between the ECAR of control and DJ-1 knock-down astrocytes, but did show the expected rotenone-induced stimulation. The data in this graph are expressed as percent control relative to OCR/GFAP values from same-time no rotenone control wells on the same plates. For interpretation of the references to color in this figure legend, the reader is referred to the Web version of this article.